AIAA JOURNAL
Vol. 47, No. 8, August 2009

Technical Notes

Extension of the Shear-Lag Solution for Structurally Attached Ultrasonic Active Sensors

Victor Giurgiutiu* and Giola Bottai-Santoni†
University of South Carolina, Columbia, South Carolina 29208

DOI: 10.2514/1.43946

I. Introduction

THIS Technical Note presents an extension to Crawley and and deLuis's [1] shear-lag solution describing the stress and strain transfer between a structurally attached piezoelectric wafer active sensor (PWAS) and the support structure.

Crawley and deLuis [1] developed an analytical model of the coupling between wafer piezoelectric actuators and thin-wall structural members. The configuration studied was of two piezoelectric elements bonded on both sides of an elastic structure. They assumed that the strain distribution in the piezoelectric actuator was a linear distribution across the thickness (Euler–Bernoulli linear flexural or uniform extension) and developed a shear-lag solution for the interfacial stress τ between the PWAS and the structure. The shear-lag parameter Γ was found to depend on modal repartition number α, which took the value $\alpha = 1$ for symmetric (i.e., axial) excitation and $\alpha = 3$ for antisymmetric (i.e., flexural) excitation. This initial analysis was further detailed by Crawley and Anderson [2]. Giurgiutiu [3] extended Crawley and deLuis's [1] and Crawley and Anderson's [2] theories to the case of only one piezoelectric element bonded to the thin-wall structure by calculating the total effect as a superposition of symmetric and antisymmetric contributions and found the value of α for a single-sided PWAS excitation to be $\alpha = 4$.

Refinements of Crawley and deLuis's [1] and Crawley and Anderson's [2] approaches have been reported in [4–6]. Luo and Tong [4] and Tong and Luo [5] studied both static and dynamic solutions of a piezoelectric smart beam and introduced the peel stress effect, but still within the limitations of the Euler–Bernoulli theory of bending. Ryu and Wang [6] analyzed the interfacial stress induced by a surface-bonded piezoelectric actuator on a curved beam. They used the variational principle to derive the governing equations and the boundary conditions, but did not seem to go beyond axial-flexural combination.

In this Technical Note, we propose to overcome the limitations of the current shear-lag model and derive a generic solution for the ultrasonic excitation transmitted between a PWAS and a thin-wall structure through an adhesive layer in the presence of multiple guided Lamb-wave modes. For the case of two generic modes, we will derive a closed-form solution that is a direct extension to the ultrasonic frequencies of Crawley and deLuis's [1] and Crawley and Anderson's [2] solutions for low frequencies.

Received 20 February 2009; revision received 17 April 2009; accepted for publication 17 April 2009.

*Professor, Mechanical Engineering Department, 300 Main Street; victorg@sc.edu.

†Ph.D. Candidate, Mechanical Engineering Department, 300 Main Street.

II. Classic Solution

Figure 1a shows how ultrasonic excitation would transmit from a PWAS into a thin-wall structure through an interfacial bonding layer; our aim is to understand how this excitation is distributed into the various guided-Lamb-wave modes existing in the structure. Assume that the PWAS has thickness t_a, half-length a, and elastic modulus E_a; the structure has thickness $t = 2d$ and elastic modulus E; and the bonding layer has thickness t_b and shear modulus G_b.

Crawley and deLuis [1] and Crawley and Anderson [2] analyzed this situation under the assumption that only axial and flexural waves exist in the structure. Equilibrium of the infinitesimal PWAS element, shown in Fig. 1a, gives $t_a\sigma_a' - \tau = 0$, where $\sigma_a = E_a(\varepsilon_a - \varepsilon_{\text{ISA}})$ is the stress in the PWAS. The piezoelectrically induced strain $\varepsilon_{\text{ISA}} = d_{31}V/t_a$ (where V is the applied electric voltage and d_{31} is the piezoelectric constant) is constant along the PWAS. Differentiation and substitution yields $t_aE_a\varepsilon_a' - \tau = 0$. Pure-shear analysis of the bonding layer yields

$$\tau = G_b\gamma = G_b(u_a - u)/t_b \tag{1}$$

Double differentiation of Eq. (1) yields $\varepsilon_a' = (t_b/G_b)\tau'' + \varepsilon'$. Substituting it into the equilibrium expression yields

$$t_aE_a(t_b/G_b)\tau'' + t_aE_a\varepsilon' - \tau = 0 \tag{2}$$

Equation (2) contains both τ and ε, we can use equilibrium in the structure to express it only in terms of τ. Consider an infinitesimal structural element of length dx (Fig. 2); analyze the equilibrium between the external shear stress $\tau(x)$ and the stress resultants N_x and M_z defined as

$$\begin{cases} N_x(x) = \int_{-d}^{+d} \sigma(x,y)\mathrm{d}y \\ M_z(x) = \int_{-d}^{+d} \sigma(x,y)y\mathrm{d}y \end{cases} \tag{3}$$

where $\sigma(x,y)$ is the total stress in the structure. Equilibrium of the infinitesimal element yields

$$\begin{cases} N_x' + \tau = 0 \\ M_z' + \tau d = 0 \end{cases} \tag{4}$$

Crawley and deLuis [1] and Crawley and Anderson [2] assumed that the total stress in the structure is a superposition of symmetric (axial) and antisymmetric (flexural) stresses that have constant and linear displacement distributions across the thickness, respectively; that is,

$$\sigma(x,y) = \sigma^S(x,y) + \sigma^A(x,y) = \sigma_{\text{ax}}(x) + (y/d)\sigma_{\text{flex}}(x)$$

where $\sigma_{\text{ax}}(x)$ and $\sigma_{\text{flex}}(x)$ are the amplitudes of the axial and flexural waves at the structural surface. Substitution of Eq. (3) into Eq. (4) and use of stress expression yields $t\sigma_{\text{ax}}'(x) + \tau(x) = 0$ and $t\sigma_{\text{flex}}'(x) + 3\tau(x) = 0$. Addition of the two equations gives

$$-t\sigma'(x,d) = \tau(x) + 3\tau(x) = 4\tau(x) = \alpha\tau(x) \tag{5}$$

where $\alpha = 4$ and $\sigma'(x,d) = \sigma_{\text{ax}}'(x) + \sigma_{\text{flex}}'(x)$. Using $\sigma = E\varepsilon$ in Eq. (5) yields the structural strain rate at the upper surface as $\varepsilon' = \alpha\tau/Et$; substitution into Eq. (2) yields the ODE in τ only: that is,

$$\tau''(x) - \Gamma^2\tau(x) = 0 \tag{6}$$

where $\Gamma^2 = (G_b/t_bt_aE_a\psi)(\psi + \alpha)$ is the shear-lag parameter and $\psi = Et/E_at_a$ is the stiffness ratio between the structure and PWAS. Equation (6) accepts solution of the form

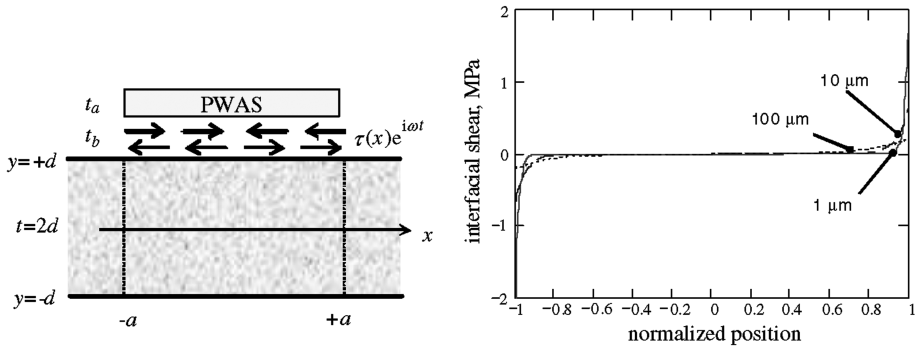

Fig. 1 PWAS and structure interaction through the interface layer: a) analysis model and b) predicted interfacial shear stress $\tau(x)$ for various interfacial thickness values [7].

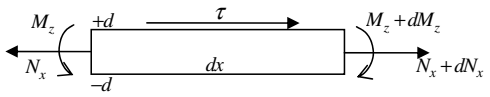

Fig. 2 Equilibrium of an infinitesimal structural element.

$$\tau(x) = c_1 \sinh \Gamma x + c_2 \cosh \Gamma x$$

where constants c_1 and c_2 are to be determined from the boundary conditions. Because the strain at the PWAS tips is $\varepsilon_{\mathrm{ISA}}$, whereas the strain in the structure at the same location is zero, and because the shear stress in the adhesive layer is $\gamma = (u_a - u)/t_a$, it follows that the boundary conditions are

$$\tau'(\pm a) = G_b \gamma'(\pm a) = G_b \varepsilon_{\mathrm{ISA}}/t_b$$

Solution of the resulting algebraic system for c_1 and c_2 yields the shear-lag solution:

$$\tau(x) = (G_b \varepsilon_{\mathrm{ISA}} a / t_b \Gamma a \cosh \Gamma a) \sinh \Gamma x \tag{7}$$

The shear-lag parameter Γ depends on α; the value of α depends on how the wave modes are excited. If two PWAS are installed, as in [1], and only axial wave is excited then $\alpha = 1$; if only the flexural wave is excited, then $\alpha = 3$. If a single PWAS is present (Fig. 1), then $\alpha = 4$, because both axial and flexural waves are equally excited [3]. Should the PWAS be placed at a different position within the thickness, then a different value of α is possible. The interfacial shear stress concentrates about the PWAS edges as the bond layer becomes thinner (or stiffer) (Fig. 1b), this leads to the *ideal-bonding* model, in which the shear transfer is assumed to be localized at the PWAS edges (i.e., represented by the Dirac δ function).

Equation (7) has been used by many investigators [3,7–17]. Although Eq. (7) is only valid at low frequency–thickness product values in which the axial/flexural wave approximation holds, many investigators have also used it at high ultrasonic frequencies [3,7–17]. However, this shear-lag model has several limitations: The theory supporting Eq. (7) assumes linear strain distribution across the thickness (i.e., constant for axial waves and gradient for flexural waves). This assumption only applies for low values of the frequency–thickness product in which S0 and A0 can be approximated with simple axial and flexural waves. The nonlinear strain distribution across the thickness of actual S0 and A0 modes would lead to different values of α, but current analysis does not consider nonlinear strain distribution. As frequency increases, more modes appear in the guided-wave structure in addition to the S0 and A0 modes, but current theory cannot accommodate more than two wave modes.

We have been able to develop a closed-form solution for the case of a symmetric and an antisymmetric nonlinear mode and two generic guided-wave modes. We have also been able to set up the general problem for an arbitrary number of nonlinear modes; in this case, a closed-form solution does not seem possible; hence, an iterative solution methodology is needed that will be presented in future communications.

III. Extension to the Case of a Symmetric and an Antisymmetric Nonlinear Mode

Assume a symmetric nonlinear mode $\sigma_S(y)$ and an antisymmetric nonlinear mode $\sigma_A(y)$ acting together; the total stress is given by superposition:

$$\sigma(x, y) = a_S(x)\sigma_S(y) + a_A(x)\sigma_A(y)$$

where $a_S(x)$ and $a_A(x)$ are x-dependent modal participation factors. At the upper surface, the stress derivative with respect to x is

$$\sigma'(x, d) = a'_S(x)\sigma_S(d) + a'_A(x)\sigma_A(d)$$

Equation (4) now becomes

$$\begin{cases} N_x(x) = t\Lambda_S a_S(x) \\ M_z(x) = td\Lambda_A a_A(x) \end{cases} \tag{8}$$

where

$$\Lambda_S = \frac{1}{t}\int_{-d}^{+d} \sigma_S(y)\mathrm{d}y$$

and

$$\Lambda_A = \frac{1}{td}\int_{-d}^{+d} \sigma_A(y) y \mathrm{d}y$$

Note that the axial force depends only on the symmetric mode and the bending moment depends only on the antisymmetric mode. Substitution of Eq. (8) into Eq. (4) yields, after some rearrangement,

$$\begin{cases} ta'_S(x) + \Lambda_S^{-1}\tau(x) = 0 \\ ta'_A(x) + \Lambda_A^{-1}\tau(x) = 0 \end{cases} \tag{9}$$

Multiplication of the first line of system (9) by $\sigma_S(d)$ and of the second line by $\sigma_A(d)$ followed by addition and rearrangement of the terms yields an equation similar to Crawley and Deluis's [1] Eq. 5: that is, $-t\sigma'(x, d) = \alpha\tau(x)$ where

$$\alpha = (\Lambda_S)^{-1}\sigma_S(d) + (\Lambda_A)^{-1}\sigma_A(d) \tag{10}$$

Equation (10) represents the extension of Crawley and Deluis's [1] solution for the case of nonlinear symmetric and antisymmetric modes. It could be used to accurately calculate the shear-lag parameter Γ of Eq. (6) at ultrasonic frequencies at which the linearity condition implied in Crawley and Deluis's formulation no longer applies. Substitution of Eq. (10) into Eq. (6) yields

$$\Gamma^2 = (G_b/t_b t_a E_a \psi)[\psi + (\sigma_S(d)/\Lambda_S) + \sigma_A(d)/\Lambda_A] \tag{11}$$

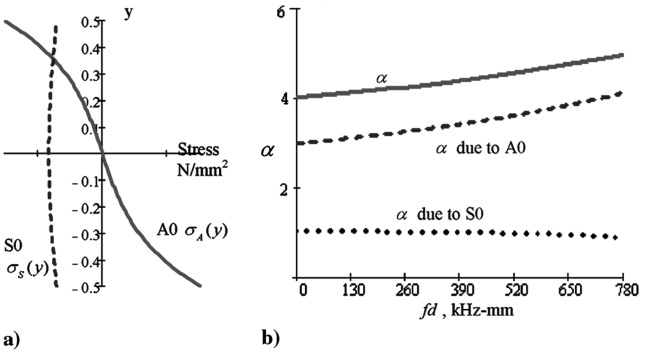

Fig. 3 Plots of a) S0 and A0 Lamb-wave modes at 700 Hz · mm for an aluminum 2024 plate and b) variation of α with frequency–thickness product fd.

To ascertain the relative importance of Eq. (10), we have plotted it for the case of a symmetric S0 and an antisymmetric A0 mode acting together at ultrasonic frequencies (Fig. 3). For aluminum 2024, for frequencies below 782 kHz mm, only the S0 and A0 modes exist and the theory presented in this section, i.e., Eq. (10) applies. Figure 3a shows the Lamb-wave mode shapes at 700 kHz mm; it is apparent that the modes have become significantly nonlinear (i.e., Crawley and Deluis's [1] initial assumptions no longer apply). Figure 3b shows the variation of α as calculated with Eq. (10). It is apparent that at low frequencies, Crawley and Deluis's value $\alpha = 1 + 3 = 4$ applies. It is apparent from Fig. 3b that as fd increases, α also increases: from $\alpha = 4$ at low frequencies to $\alpha \simeq 5$ at high frequencies. It is also interesting to observe that at high frequencies, the relative contribution of S0 and A0 changes, with S0 contribution decreasing and A0 contribution increasing.

IV. Extension to the Case of Two Generic Guided-Wave Modes

In the case of two generic modes, we will derive an expression for the shear-lag parameter Γ to be used directly in the shear-lag solution (7). Assume two generic guided-wave modes, then

$$\sigma(x, y) = a_1(x)\sigma_1(y) + a_2(x)\sigma_2(y)$$

where $a_1(x)$ and $a_2(x)$ are x-dependent modal participation factors. At the upper surface, $y = d$, the stress derivative with respect to x is

$$\sigma'(x, d) = a_1'(x)\sigma_1(d) + a_2'(x)\sigma_2(d) \tag{12}$$

Substitution of Eq. (3) into Eq. (4) and use of Eq. (12) yields

$$\begin{cases} N_x(x) = t[\Lambda_1^S a_1(x) + \Lambda_2^S a_2(x)] \\ M_z(x) = td[\Lambda_1^A a_1(x) + \Lambda_2^A a_2(x)] \end{cases} \tag{13}$$

$$\begin{cases} \Lambda_n^S = (1/t)\int_{-d}^{+d} \sigma_n(y)\mathrm{d}y \\ \Lambda_n^A = (1/td)\int_{-d}^{+d} \sigma_n(y)y\mathrm{d}y \end{cases} \qquad n = 1, 2 \tag{14}$$

Substitution of Eq. (13) into Eq. (4) yields a system of two equations into two unknowns: $a_1'(x)$ and $a_2'(x)$. Using the solutions of the system and substituting Eq. (12) into Eq. (2) yields Eq. (6), but with a more general expression of Γ given by

$$\Gamma^2 = \frac{G_b}{E_a t_b t_a \psi}\left[\psi + \frac{(\Lambda_2^S - \Lambda_2^A)\sigma_1(d)}{\Lambda_1^A\Lambda_2^S - \Lambda_1^S\Lambda_2^A} + \frac{(\Lambda_1^S - \Lambda_1^A)\sigma_2(d)}{\Lambda_1^S\Lambda_2^A - \Lambda_1^A\Lambda_2^S}\right] \tag{15}$$

Equation (15) can be applied to any two modes, at any frequency, and of arbitrary thickness distribution. It can be easily verified that Eq. (15) is asymptotically consistent with the low-frequency solution of Eq. (6). In fact, Eq. (15) reduces to Eq. (11) if the two generic modes are symmetric and antisymmetric modes, respectively [Eq. (14) yields $\Lambda_1^S = \Lambda_S$, $\Lambda_2^S = \Lambda_1^A = 0$, and $\Lambda_2^A = \Lambda_A$]. Moreover, it has already been shown that Eq. (11) is asymptotically consistent with Crawley and Deluis's [1] low-frequency solution.

V. Extension to the Case of N Generic Guided-Wave Modes

In this section, we will tackle the situation of N generic nonlinear guided-wave modes. It will be shown that the closed-form solutions as achieved in previous sections are no longer possible. Assume the general solution to be a superposition of N guided-wave modes: that is,

$$\sigma(x, d) = \sum_{n=1}^{N} a_n(x)\sigma_n(d) \tag{16}$$

Substitution of Eq. (3) into Eq. (4) and use of Eq. (16) yields

$$N_x(x) = t\sum \Lambda_n^S a_n(x)$$

and

$$M_z(x) = td\sum \Lambda_n^A a_n(x)$$

where Λ_n^S and Λ_n^A, for $n = 1, \ldots, N$, are defined in Eq. (14). Equation (4) now becomes

$$\begin{cases} t\sum_n^N \Lambda_n^S a_n'(x) + \tau(x) = 0 \\ t\sum_n^N \Lambda_n^A a_n'(x) + \tau(x) = 0 \end{cases} \tag{17}$$

For two generic modes ($N = 2$), the linear system (17) can be solved for $a_n'(x)$ ($n = 1, 2$), as we showed in Sec. IV. For N generic modes, system (17) has two equations with N unknowns (i.e., it is $N - 2$ indeterminate). We use the normal mode-expansion method to derive the interfacial shear stress. Recall the generic expression of forward (+) and backward (−) moving guided waves under surface shear excitation $\tau(x)$ ($-a \le x \le a$) [18] (page 210, Eqs. 14–21); that is,

$$a_n^{\pm}(x) = \pm\frac{\tilde{v}_x^n(d)e^{\mp i\xi_n x}}{4P_{nn}}\int_{\mp a}^{x} e^{\pm i\xi_n \bar{x}}\tau(\bar{x})\mathrm{d}\bar{x} \tag{18}$$

where ξ is the wave number, $v_i^n(y)$ is the velocity vector of the nth mode, tilde ($\sim$) signifies complex conjugate, and P_{nn} is the power flow in the nth mode. Substitution of Eq. (18) into Eq. (16) and division by E yields

$$\varepsilon'(x) = E^{-1}\left[\sum_{n=1}^{N} a_n'^{+}(x)\sigma_n(d) + \sum_{n=1}^{N} a_n'^{-}(x)\sigma_n(d)\right] \tag{19}$$

Substitution of Eq. (19) into Eq. (2) yields an the integro-differential equation for $\tau(x)$: that is,

$$\tau''(x) - \Gamma^2\tau(x) - i\left(\frac{G_b}{t_b E}\right)\sum_{n=1}^{N}\xi_n[a_n^+(x) + a_n^-(x)] = 0 \tag{20}$$

where

$$\Gamma^2 = \frac{G_b}{t_a t_b E_a \psi}\left[\psi - t\sum_{n=1}^{N}\frac{\tilde{v}_x^n(d)\sigma_n(d)}{4P_{nn}}\right]$$

The integro-differential Eq. (20) needs to be solved by numerical methods. This is still work in progress to be reported on in a future communication.

VI. Conclusions

The objective of this Technical Note has been to understand how ultrasonic excitation is transmitted from a PWAS into a thin-wall structure through the adhesive layer and how it is distributed into the Lamb-wave modes existing in the structure. We recalled the widely cited seminal works by Crawley and deLuis [1] and Crawley and

Anderson [2] and we noticed that their applicability is limited to low-frequency applications at which the guided-wave modes are approximated by the axial and flexural waves with their characteristic linear behavior across the thickness. We extended Crawley and deLuis's [1] and Crawley and Anderson's [2] works to nonlinear guided-wave modes. We obtained a closed-form solution for parameter α and observed that this parameter is no longer constant, but varies with the frequency–thickness product. A graph was given of this variation up to the maximum fd value for which only S0 and A0 modes exist. Changes in α of up to 25% were observed, along with redistribution of its S0 and A0 modes contributions. The theory was further extended to the case of two generic guided-wave modes for which a closed-form solution was still possible. For the case of N generic modes, a closed-form solution was no longer possible, but an iterative approach has been considered and will be reported upon in a future communication.

References

[1] Crawley, E. F., and deLuis, J., "Use of Piezoelectric Actuators as Elements of Intelligent Structures," *AIAA Journal*, Vol. 25, No. 10, 1987, pp. 1373–1385. doi:10.2514/3.9792

[2] Crawley, E. F., and Anderson, E. H., "Detailed Models of Piezoceramic Actuation of Beams," *Journal of Intelligent Material Systems and Structures*, Vol. 1, No. 1, Jan. 1990, pp. 4–25. doi:10.1177/1045389X9000100102

[3] Giurgiutiu, V., "Tuned Lamb-Wave Excitation and Detection with Piezoelectric Wafer Active Sensors for Structural Health Monitoring," *Journal of Intelligent Material Systems and Structures*, Vol. 16, No. 4, Apr. 2005, pp. 291–306. doi:10.1177/1045389X05050106

[4] Luo, Q., and Tong, L., "Exact Static Solutions to Piezoelectric Smart Beams Including Peel Stresses," *International Journal of Solids and Structures*, Vol. 39, No. 18, 2002, pp. 4677–4722. doi:10.1016/S0020-7683(02)00383-9

[5] Tong, L., and Luo, Q., "Exact Dynamic Solutions to Piezoelectric Smart Beams Including Peel Stresses," *International Journal of Solids and Structures*, Vol. 40, No. 18, 2003, pp. 4789–4836. doi:10.1016/S0020-7683(03)00264-6

[6] Ryu, D. H., and Wang K. W., "Analysis of Interfacial Stress and Actuation Authorities Induced by Surface-Bonded Piezoelectric Actuators on Curved Flexible Beams," *Smart Materials and Structures*, Vol. 13, No. 4, Aug. 2004, pp. 753–761.

[7] Giurgiutiu, V., and Lyshevski, S. E., *Micromechatronics, Micromechatronics: Modeling, Analysis, and Design with MATLAB*, CRC Press, Boca Raton, FL, 2004, p. 856.

[8] Raghavan, A., and Cesnik C. E. S., "Modeling of Piezoelectric-Based Lamb-Wave Generation and Sensing for Structural Health Monitoring," *Proceedings of SPIE: The International Society for Optical Engineering*, Vol. 5391, July 2004, pp. 419–430. doi:10.1117/12.540269

[9] Raghavan, A., and Cesnik, C. E. S., "Piezoelectric-Actuator Excited-Wave Field Solution for Guided-Wave Structural Health Monitoring," *Proceedings of SPIE: The International Society for Optical Engineering*, Vol. 5765, pp. 313–323. doi:10.1117/12.600817

[10] Lin, X., and Yuan, F. G., "Diagnostic Lamb Waves in an Integrated Piezoelectric Sensor/Actuator Plate: Analytical and Experimental Studies," *Smart Materials and Structures*, Vol. 10, No. 5, 2001, pp. 907–913. doi:10.1088/0964-1726/10/5/307

[11] Lanza di Scalea, F., Matt, H., and Bartoli, I., "The Response of Rectangular Piezoelectric Sensors to Rayleigh and Lamb Ultrasonic Waves," *Journal of the Acoustical Society of America*, Vol. 121, No. 1, 2007, pp. 175–187. doi:10.1121/1.2400668

[12] Matt, H., and Lanza di Scalea, F., "Macro-Fiber Composite Piezoelectric Rosettes for Acoustic Source Location in Complex Structures," *Smart Materials and Structures*, Vol. 16, No. 4, 2007, pp. 1489–1499. doi:10.1088/0964-1726/16/4/064

[13] Bhalla, S., and Soh, C. K., "Electromechanical Impedance Modeling for Adhesively Bonded Piezo-Transducers," *Journal of Intelligent Material Systems and Structures*, Vol. 15, No. 12, 2004, pp. 955–972. doi:10.1177/1045389X04046309

[14] Annamdas, V. G. M., and Soh, C. K., "An Electromechanical Impedance Model of a Piezoceramic Transducer-Structure in the Presence of Thick Adhesive Bonding," *Smart Materials and Structures*, Vol. 16, No. 3, 2007, pp. 673–686.

[15] Dugnani, R., "Dynamic Behavior of Structure-Mounted Disk-Shape Piezoelectric Sensors Including the Adhesive Layer," *Journal of Intelligent Material Systems and Structures* (to be published).

[16] Bottai-Santoni, G., and Giurgiutiu, V., "Simulation of the Lamb Wave Interaction Between Piezoelectric Wafer Active Sensors and Host Structure," *Proceedings of SPIE: The International Society for Optical Engineering*, Vol. 5765, 2005, pp. 259–270. doi:10.1117/12.597747

[17] Giurgiutiu, V., *Structural Health Monitoring with Piezoelectric Wafer Active Sensors*, Elsevier, New York, 2008, p. 760.

[18] Rose, J. L., *Ultrasonic Waves in Solid Media*, Cambridge Univ. Press, New York, 1999.

A. Palazotto
Associate Editor